THE AMERICAN SOCIETY OF MECHANICAL ENGINEERS
345 E. 47th St., New York, N.Y. 10017

97-GT-249

THE EFFECTS OF FATIGUE CRACKS ON FREE TORSIONAL VIBRATION OF SHAFTS

H. -Y. Yen
M. -H. Herman Shen*
Department of Aerospace Engineering,
Applied Mechanics, and Aviation
The Ohio State University
Columbus, Ohio 43210-1276

ABSTRACT

The effect of a single-edge fatigue crack on the torsional vibration of shafts is investigated. A generalized variational principle is used to formulate the equation of motion and associated boundary conditions for the free vibration of a nonrotating shaft with a fatigue crack of arbitrary size and location. The fatigue crack is introduced in the form of a single-edge crack. The stress and strain of the cracked shaft are determined by introducing a crack function and a displacement function into the shaft's compatibility relations. The crack function is designed to have the maximum value at the cracked section and decay exponentially away from the crack along the shaft's longitudinal direction. A displacement function is constructed to modify the in-plane displacement and its slope near the single-edge crack. The natural response of the free-free shaft is calculated through a Galerkin procedure. The results indicated a clear change in the natural frequencies of the cracked nonrotating shaft.

[1]to whom correspondence should be addressed, ASME member.

NOMENCLATURE

$a = a(z)$	crack length
b	half breadth of shaft
d	half depth of shaft
L	length of shaft
E	Young's Modulus of Elasticity
G	Shear Modulus of Elasticity
J	polar moment of area of shaft section
m	stress magnification factor
p_i	momentum components
W_0	natural frequency
LR	the ratio of the crack location
u, v, w	displacement components
$\bar{u}_i$	prescribled surface displacements
Φ	assumed shaft shape function
X, Y, Z	hody function
α	exponential decay constant
σ_{ij}	stress components
ϵ_{ij}	strain components
δ_{ij}	Kronecker's delta
θ	angular displacement
λ	Lame's constant
ν	Poisson's ratio
ρ	density

Presented at the International Gas Turbine & Aeroengine Congress & Exhibition
Orlando, Florida — June 2–June 5, 1997

INTRODUCTION

Fatigue cracking is one of the most destructive types of damage to in-service structural systems such as turbines, generators, and motors. Since these structures are optimally designed and operate under severe conditions, any damage that does not receive immediate attention may lead to failure of the entire system. Therefore, in order to ensure safety and reliability, on-line health monitoring is becoming an essential issue in modern in-service structural system configuration designs such as aircraft gas turbine engines. This type of health monitoring system demands a high degree of efficiency, accuracy, and durability for detecting and identifying damage in real time or quasi-real time.

A number of on-line structural health monitoring methods have been proposed for in-service structures in past decades. Among these methods, damage identification approaches based upon dynamic response has received much attention and has been widely developed. The fundamental concept in the dynamic response based damage detection approach is primarily concerned with the determination of the *properties* of the damage (e.g. crack size and location) from the changes of the on-line *behavior* such as natural frequencies, mode shapes, dynamic responses, etc. This can be achieved by constructing a mathematical model for structures containing fatigues cracks, and is the motivation for recent studies of the dynamics of cracked structures such as beams and shafts.

Dynamics of cracked structures in one dimensional vibrating continuous structures can be separated into two categories: simple torsional vibrations and bending vibrations. The vibration of cracked beams was first studied by Christides and Barr (1984) based on simple beam theory. They derived the equation of bending motion for a Euler-Bernoulli beam with pairs of symmetric cracks. An exponential-type function (the so-called crack function) was used to model the stress concentration near the crack-tip. Shen and Pierre (1990) found that Christides and Barr's (1984) two-term Ritz solution was not fully converged and hence a modified Galerkin expansion was suggested in order to improve the solution. In addition, Shen and Pierre (1990) proposed a 2-D finite element approach to determine/re-evaluate the parameter that controls the stress concentration profile.

Shen and Pierre later extended the theory to beams with single-edge cracks (1994) by using the generalized variational principle which allows for modified stress/strain and displacement fields for the compatibility requirements. The concentration in stress was medeled by introducing the crack function as proposed by Christides and Barr (1984). Most importantly, a displacement function was also proposed by Shen and Pierre (1994) to modify the in-plane displacement and its slope near the single-edge crack. Christides and Barr (1986) also derived the equation of torsional motion for a beam containing pairs of symmetrical cracks by a similar procedure (Christides and Barr, 1984), but the rate of stress decay was evaluated via the experimental data.

The objective of this research is to investigate the torsional dynamic behavior of shafts with single-edge fatigue cracks, and an attempt is presented to extend the continuous cracked beam theory proposed originally by Christides and Barr (1984) and later modified by Shen and Pierre (1990, 1994) for the torsional vibration of nonrotating shafts containing a single-edge fatigue crack. First, the modeling of the cracked shaft is approached in a more fundamental way with the intention of retaining the framework of a one-dimensional elastic continuum. In modeling the fatigue crack, effort is focused on obtaining the governing equation of cracked shafts by using the crack function proposed by Christides and Barr (1986) and the displacement function proposed by Shen and Pierre (1994). The equation of motion and associated boundary conditions for the free vibration of a nonrotating shaft with a fatigue crack of arbitrary size and location are formulated through a generalized variational principle. The natural response of the free-free rotating shaft is calculated by using a Galerkin approach. The results indicated a clear change in the natural frequencies of the cracked nonrotating shaft, and the effect of a single-edge fatigue crack on the torsional vibration of nonrotating shafts is discussed.

THEORETICAL DEVELOPMENT

For an uncracked shaft, torsional displacement can be defined as follows:

$$u = \phi(y,z)\theta'(x,t) \quad (1)$$

$$v = -z\theta(x,t) \quad (2)$$

$$w = y\theta(x,t) \quad (3)$$

where $\phi(y,z)$ is the warping function and u, v, and w are the displacements in the x, y, and z directions, respectively.

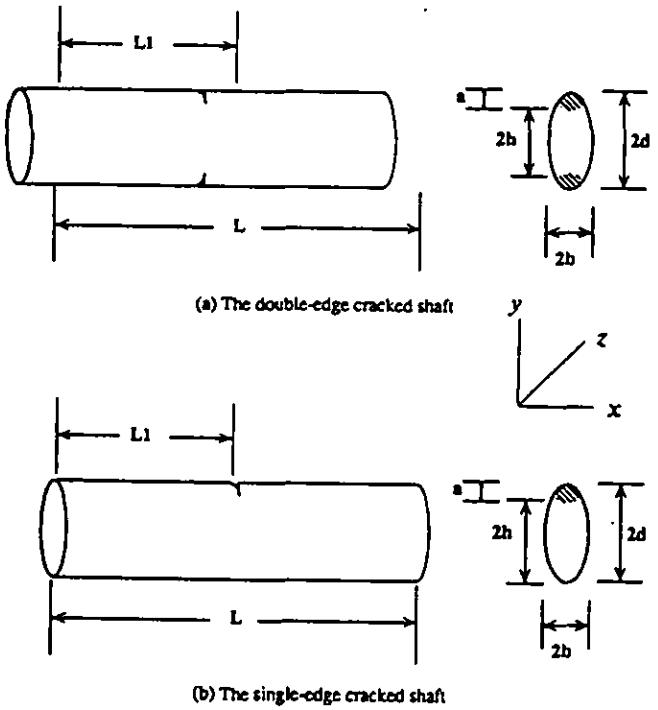

Figure 1: GEOMETRY OF A FREE-FREE SHAFT CONTAINING (A) A PAIR OF DOUBLE-EDGE CRACKS (B) A SINGLE-EDGE CRACK

Construction of Crack Functions

Double-Edge Crack - Christides and Barr (1986)

According to Christides and Barr's (1986) assumptions for a cracked beam in torsional vibration, the stress and strain fields of the cracked beam can be obtained by adding perturbation functions to the stress and strain distributions of the undamaged beam. These functions have their maximum value at the tip of the crack and decay with distance from the cracked section. Thus, the perturbation in the direct components σ_{xx} and ϵ_{xx} is introduced through a function defined as $f_1(x,y,z)$, the perturbation in the shear components σ_{xy} and ϵ_{xy} is introduced through a function defined as $f_2(x,y,z)$, and the perturbation in the shear components σ_{xz} and ϵ_{xz} is introduced through a function defined as $f_3(x,y,z)$. A free-free shaft with a double-edge crack or single-edge crack is shown in Figure 1, where the pair of symmetric cracks are assumed to occur in the crack planes normal to the axis of the shaft and intersect the outer surface of the shaft. Shown in Figure 1(a) is a typical symmetrical crack situation with the crack depth a and the remaining material depth h. At the cracked section, an assumption has been made about the shear stress distribution in order to satisfy the boundary condition in which the stress distributions $(\phi + f_1)$, $(\frac{\partial\phi}{\partial y} - z + f_2)$, and $(\frac{\partial\phi}{\partial z} + y + f_2)$ are replacement by $m\phi_c$, $m(\frac{\partial\phi_c}{\partial y} - z)$, and $(\frac{\partial\phi_c}{\partial z} + y)$ at the crack tip, where ϕ_c is the warping function associated with the reduced section at the crack.

Using the unit step function, the stresses can be described as zero in the cracked zone. In the double-edge crack case, the cracked zone is between $-h$ and h. So, the unit step function becomes

$$-h < y > h \qquad H(h - |y|) = 1 \tag{4}$$

$$y < -h, y > h \qquad H(h - |y|) = 0 \tag{5}$$

Then,

$$\int_{A_r} (\cdots) dA = \int_{-h}^{h} \int_{-b}^{b} (\cdots) dz dy$$

where A_r is the cracked zone. According to the above assumptions, with the cracks at the position X_c, the perturbation functions f_1, f_2, and f_3 are taken to be

$$f_1(x,y,z) = [m\phi_c H((d-a)-y) - \phi] e^{-\alpha \frac{x - x_c}{d}} \tag{6}$$

$$f_2(x,y,z) = [m(\frac{\partial\phi_c}{\partial y} - z) H((d-a)-y) - (\frac{\partial\phi}{\partial y} - z)] e^{-\alpha \frac{x - x_c}{d}} \tag{7}$$

$$f_3(x,y,z) = [m(\frac{\partial\phi_c}{\partial z} + y) H((d-a)-y) - (\frac{\partial\phi}{\partial z} + y)] e^{-\alpha \frac{x - x_c}{d}} \tag{8}$$

where α is a positive non-dimensional constant, where $\alpha = 1.12$, which was determined from experimental results by Christide and Barr (1986).

Construction of Single-Edge Crack Functions

The above assumptions by Christides and Barr (1986) only meet the requirement for the symmetric crack. For the single-edge cracked case, the perturbation functions and the neutral axis must be modified because the cracks do not retain the symmetry of the cross-section area. A typical example for the single-edge crack as shown in Figure 1(b) is that the neutral axis is no longer a straight line at the crack tip. Therefore, the crack function f_3 will be changed to

$$f_3(x,y,z) = [m(\frac{\partial\phi_c}{\partial z} + y - \frac{a}{2}) H((d-a)-y)$$

$$-(\frac{\partial \phi}{\partial z}+y)]e^{-\alpha\frac{x-x_c}{d}} \quad (9)$$

The neutral axis y will then be replaced by

$$yy = y-(y+\frac{a}{2})H((d-a)-y)e^{-\alpha\frac{x-x_c}{d}} \quad (10)$$

The cracked zone is different from the double-edge cracked shaft, and so the unit step function need to be modified as

$$y<h \qquad H(h-y)=1 \quad (11)$$
$$y>h \qquad H(h-y)=0 \quad (12)$$

Then,

$$\int_{A_r}(\cdots)dA = \int_{-d}^{h}\int_{-b}^{b}(\cdots)dzdy$$

where A_r is the cracked zone

EQUATION OF MOTION DERIVATION

Using the equation of the extended Hu-Washizu variational principle and the various quantities from the stresses, strains, displacements, momentums, and boundary conditions, the entire variational expression for the torsion problem has been formulated. In this work, the Hu-Washizu principle is modified to include the virtual work done by the inertial forces. This yields the following functional:

$$J=\int_{t_1}^{t_2}\{\int_V[\rho p_i\dot{u}_i-\frac{1}{2}\rho p_i p_i-\underline{A}(\epsilon_{ij})+(\epsilon_{ij}-\frac{1}{2}(u_{i,j}+u_{j,i}))$$

$$\sigma_{ij}+X_i u_i]dV+\int_{S_1}\bar{g}_i u_i dS+\int_{S_2}g_i(u_i-\bar{u}_i)dS\}dt \quad (13)$$

where ρ is the mass density, $\underline{A}(\epsilon_{ij})$ is the strain energy density function, the g_i are the respective surface tractions, V is the total volume of the system, and S is its external surface.

The functional J of Eq. (13) has stationary values for the actual solution for the independent quantities u_i, p_i, ϵ_{ij}, and σ_{ij}. Therefore, from variational principle, for arbitrary independent variations of δu_i, δp_i, $\delta\epsilon_i$, and $\delta\sigma_i$, the first variation of the functional J vanishes, i.e., δJ=0, and is listed as follows:

$$\int_v\{[\sigma_{ij,j}+X_i-\rho\dot{p}_i]\delta u_i+[\sigma_{ij}-W,\epsilon_{ij}]\delta\epsilon_{ij}+[\epsilon_{ij}$$

$$-(1-\frac{1}{2}\delta_{ij})(u_{i,j}+u_{j,i})]\delta\sigma_{ij}+[\rho\dot{u}_i-T,p_i]\delta p_i\}dV$$

$$+\int_{S_p}[\bar{g}_i-g_i]\delta u_i dS+\int_{S_u}[u_i-\bar{u}_i]\delta g_i dS=0 \quad (14)$$

The variations $\delta\theta$, δS, δT, and δq are independent, so that the each expression multiplied by them in the volume integrals must be zero. Then the following relations can be given as

$$S_1 = Q_1\theta'' \quad (15)$$
$$S_2 = Q_2\theta' \quad (16)$$
$$T_1 = ES_1 = EQ_1\theta'' \quad (17)$$
$$T_2 = GS_2 = GQ_2\theta' \quad (18)$$

The equation of motion becomes

$$\eta_1 E\theta''''+2\eta_1' E\theta'''+(\eta_1'' E-\eta_2 G)\theta''-\eta_2' G\theta'$$

$$+\rho J\ddot{\theta}=0 \quad (19)$$

where η_1, η_2, Q_1, and Q_2 are defined as Christides and Barr (1986). The equation of motion is a fourth order differential equation, so that two boundary conditions must be satisfied at each end of the shaft.

The boundary conditions of the problem consist of the boundary term in the dynamic equilibrium term together with terms obtained from the surface integrals over S_p and S_u. In these integrals, the surface force obtained from the stress components $g_i=\sigma_{ij}n_j$, and force obtained from the stress components, $g_i=\sigma_{ij}n_j$, where n_j is the direction cosine of the surface normal.

Considering the ends of the shaft to be plane and normal to the longitudinal axis, the direction cosines are $\nu_x=-1$ at $x=0$ and $\nu_x=1$ at $x=l$. Additional, ν_y and ν_z are zero at both ends. Then, $g_x=\pm\sigma_{xx}$, $g_y=\pm\sigma_{xy}$, and $g_z=\pm\sigma_{xz}$ Also, if the specified forces $\bar{g}_i$ at the ends are $\bar{X}$, $\bar{Y}$, or $\bar{Z}$, the boundary condition obtained by integrating over the surface S_p becomes

$$[\int_A\{(\bar{X}-\sigma_{xx})\delta u+(\bar{Y}-\sigma_{xy})\delta v+(\bar{Z}-\sigma_{xz})\delta w\}dA]_{x=l}$$

$$+[\int_A\{(\bar{X}+\sigma_{xx})\delta u+(\bar{Y}+\sigma_{xy})\delta v+(\bar{Z}+\sigma_{xz})\delta w\}dA]_{x=0} \quad (20)$$

On the other hand, for the precrihed displacements, the surface S_u integral of the variational equation over the ends $x=0$ and $x=L$ is

$$[\int_A\{(u-\bar{u})\delta\sigma_{xx}+(v-\bar{v})\delta\sigma_{xy}+(w-\bar{w})\delta\sigma_{xz}\}dA]_{x=l}$$

$$-[\int_A\{(u-\bar{u})\delta\sigma_{xx}+(v-\bar{v})\delta\sigma_{xy}+(w-\bar{w})\delta\sigma_{xz}\}dA]_{x=0} \quad (21)$$

where $\bar{u}$, $\bar{v}$ and $\bar{w}$ are the prescribed displacements at the ends of the shaft.

GALERKIN'S SOLUTION

The differential equation including the dynamic equilibrium term is

$$[\eta_1 E\theta'']'' - (\eta_2 G\theta')' = \rho J\ddot{\theta} \qquad (22)$$

A free-free shaft is shown in Figure 1 with a crack at a distance L_1 from the left end. The mode shapes are defined as

$$\theta(x,t) = \sum_{i=1}^{\infty} a_i(t)cos[i\pi(\frac{x}{l})] \qquad (23)$$

$$\Phi(x,t) = \sum_{j=1}^{\infty} \Phi_i(t)cos[j\pi(\frac{x}{l})] \qquad (24)$$

where $a(t)$ is assumed functions of time, and $\Phi(x,t)$ is a shape function. Substituting (23) and (24) into (22), and applying Galerkin's method yields a discritized eigenvalue problem

$$[K]n - W_0^2[M]n = 0 \qquad (25)$$

where n is the generalized coordinates. In this example, ten comparison functions are selected in the Galerkin's procedure. Therefore, the shaft deflection which is expanded in such a series of comparison functions not only improves the results as compared to those given by Christides and Barr (1986), but also predicts the higher natural modes. Although the mode of the cracked shaft has a discontinuous fourth derivative, the Galerkin expansion only requires a small number of terms, such as ten terms, to satisfy the convergence criterion.

Applying the Galerkin procedure, the equation of motion becomes

$$\int_0^l \{cos[j\pi(\frac{x}{l})][\eta_1 E\sum_{i=1}^{n} a_i(t)(-\frac{i^2\pi^2}{l^2}cos[i\pi(\frac{x}{l})])]''$$

$$-cos[j\pi(\frac{x}{l})][\eta_2 G\sum_{i=1}^{n} a_i(t)(-\frac{i\pi}{l}sin[i\pi(\frac{x}{l})])]'\}dx$$

$$+W_0^2\int_0^l \{\rho J cos[j\pi(\frac{x}{l})]\sum_{i=1}^{n} a_i(t)cos[i\pi(\frac{x}{l})]\}da = 0 \qquad (26)$$

Integrating by parts over the x direction and solving the above eigenvalue problem, the $(i,j)th$ element of stiffness matrix $[K]$ can be taken as

$$[K] = \frac{ij\pi^2}{l^2}\{(\frac{ij\pi^2}{l^2})E\int_0^l \eta_1 cos[i\pi(\frac{x}{l})]cos[j\pi(\frac{x}{l})]dx$$

$$+G\int_0^l \eta_2 sin[i\pi(\frac{x}{l})]sin[j\pi(\frac{x}{l})]dx\} \qquad (27)$$

and the mass matrix $[M]$ becomes

$$[M] = \int_0^l \rho J cos[i\pi(\frac{x}{l})]cos[j\pi(\frac{x}{l})]dx \qquad (28)$$

The Galerkin method also provides full convergence for the stiffness and mass matrix. Even if using a 50-vector of the generalized coordinates to compute the matrix, the natural frequency of the cracked shaft W_0 would be nearly the same as these 10-vector of the generalized coordinates, which is much more stable than a two-term Rayleigh-Ritz solution, such as Christides and Barr's solution.

RESULTS AND DISCUSSION

The following examples of free torsional vibration analysis of cracked shafts were constructed. These examples, as shown in Figure 1 (a) and (b), are of a nonrotating shaft containing a pair of double-edge cracks or a single-edge crack.

The first case corresponds to the study of natural response of free-free nonrotating cracked shafts with a pair of double-edge cracks at mid-span symmetric with respect to the neutral axis and perpendicular to it. The solution of the Galerkin procedure is shown in Table 1, which consists of the first and third natural frequencies only. The third and fifth columns show the first and third natural frequency ratio (FR), the ratio of the natural frequency of the cracked shaft to that of the uncracked shaft. In order to validate the Galerkin predictions, the second and fourth columns presented the first and third natural frequency ratio obtained from Christides and Barr's experimental data (1986). The results in Table 1 clearly indicate that the proposed analytical predictions in natural frequencies agree with the experimental data.

The effects of mid-span symmetric cracks on the first mode frequency is shown in Figure 2. The experimental results agree very well with the present Galerkin solution for crack ratios up to 0.6. On the other hand, the decrease in frequency predicted by the Galerkin solution for crack ratio greater than 0.6 does not agree as well with the experimental results. This might be caused by the assumption that the slope of stress in the z direction is a linear distribution at the cracked section instead of $\frac{1}{\sqrt{r}}$, where r is the distance from the crack tip in the real case.

In the second example, we examined the effect of crack position on the sensitivity of natural frequencies

of free-free nonrotating shafts with a single-edge crack. The first torsional frequency is shown in Figure 3 as a function of the crack ratio for four crack positions, LR=0.125, 0.25, 0.375, and 0.5, where $LR = L1/L$ is the normalized crack location. The drop in frequency is far greater for cracks near the mid-span, while the frequency is almost unchanged when crack is located near the free ends. This result can be explained by noting that the torsional moment is distributed heavily near the mid-span for the first mode, leading to a severe loss in torsional stiffness due to the crack.

However, the drop in frequency is different in the higher modes. The solid curves in Figure 3 show that the second frequency is relatively much less affected than the first for LR=0.5, but strongly affected for other crack locations such as LR=0.25. In other words, the frequency drop is greatest for cracks located where the torsional moment is largest. The reason for this is that the second mode torsional vibration is an antisymmetrical mode vibration. Hence, the drop of the second mode frequency is unnoticeable at mid-span as shown by the solid line.

The third mode frequency drop in terms of crack depth is shown in Figure 3. As we expect, the sensitivity to the crack position is very similar to the first mode case, but a more noticeable drop occurs as the crack size increases.

The mode shapes obtained by the Galerkin formulation of the single-edge cracked shaft are compared in Figure 4. One observation from these three plots is that the prediction of the crack's location and depth based upon only one mode could be misleading. For instance, by reviewing only the second mode shape, one would conclude that the shaft is not damaged. This implies that different modes viewed separately might yield different predictions of damages, i.e., crack position and depth. Moreover, the effect on the third mode sbape is more severe than on the first.

From the above discussion, the sensitivity to cracks depends highly on the mode number and the crack location. Several observations can be made from this study. First, for a given mode, the effects on the torsional frequency and mode shape become more severe as the crack depth increases. Second, for a particular crack ratio, the crack position strongly affects the dynamic behavior of a cracked shaft. Third, if the position of the crack is known, one specific mode may be sufficient to obtain accurate results in the crack identification problem. On the other hand, if the crack position is unknown, the uniqueness and accuracy of the identification process becomes questionable. In general, if more modes are used for crack identification, more accurate and reliable results can be achieved.

Table 1: COMPARISON OF GALERKIN'S SOLUTION AND CHRISTIDES AND BARR'S EXPERIMENTAL RESULTS

$(\frac{a}{d})$	$(\frac{P_c}{P_i})$(CB)	$(\frac{P_c}{P_i})$(A)	$(\frac{P_c}{P_{sc}})$(CB)	$(\frac{P_c}{P_{sc}})$(A)
0.000	1.000	1.000	1.000	1.000
0.079	0.998	0.996	0.999	0.996
0.157	0.996	0.992	0.998	0.992
0.236	0.992	0.986	0.994	0.988
0.315	0.988	0.980	0.988	0.982
0.394	0.979	0.972	0.981	0.976
0.472	0.969	0.961	0.967	0.967
0.551	0.954	0.947	0.951	0.956
0.630	0.939	0.926	0.937	0.942
0.709	0.904	0.893	0.908	0.922
0.787	0.866	0.835	0.871	0.891
0.866	0.807	0.714	0.829	0.845
0.965	0.678	0.442	0.763	0.772
1.000	0.000	0.000	0.000	0.000

CB: Christides and Barr's experimental results
A: Analytical results

CONCLUSIONS

In the present study, the equation of motion has been derived for nonrotating shafts containing a single-edge crack. By applying the Galerkin procedure, the approximate equation of motion for first three mode has been ohtained in single-edge crack. It leads that the torsional frequency and mode shape can be used as one of the tools to predict the crack location and crack size of the shaft. Also, this analytical solution shows excellent agreement with experimental results and finite element predictions.

Further study on the analytical solution of a cracked shafts is considered the rotating situation, and the effect of the rotatind speed. Also, considering the torsion coupled with bending motion will be another task of the authers. Hopefully, the solution can provide more accurate identification process of the cracked shaft.

REFERENCES

S. Christides and A. D. S. Barr 1984 "One-dimensional Theory of Cracked Bernoulli-Eular Beams," *International Journal of the Mechanical Sciences* 26, pp. 639-648.

S. Christides and A. D. S. Barr 1986 "Torsional Vibration of Cracked Beams of Non-Circular Cross-Section," *International Journal of the Mechanical Sciences* 28, pp. 473-490.

M.-H. H. Shen and C. Pierre 1990 "Natrual modes of Bernoulli-Eular Beams with Symmetric Crack," *Journal of Sound and Vibration* 138, pp. 115-134.

M.-H. H. Shen and C. Pierre 1994 "Free Vibratinns of Beams with A Single-Edge Crack," *Journal of Sound and Vibration* 170, pp. 237-259.

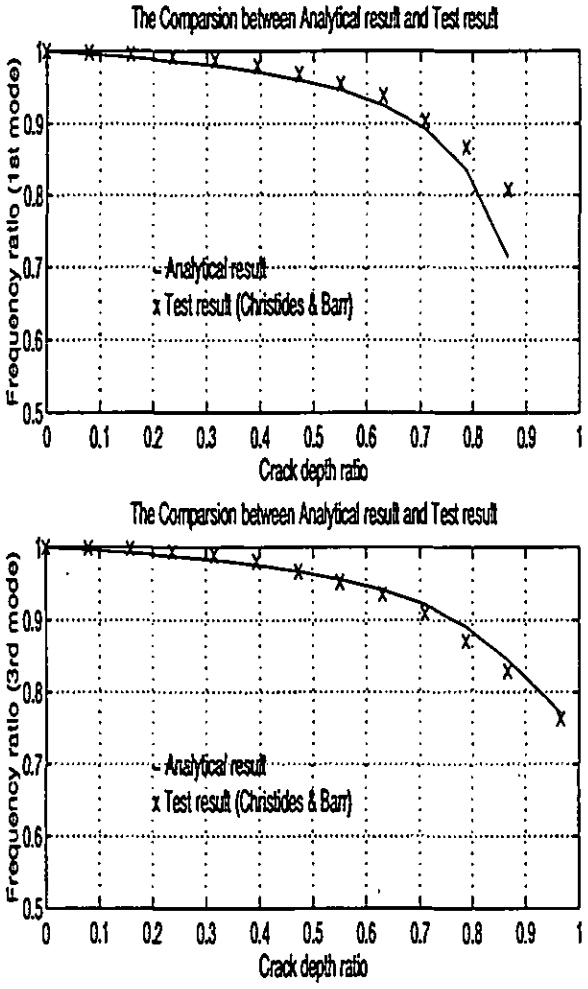

Figure 2: THE NATURAL FREQUENCY OF A FREE-FREE SHAFT WITH A PAIR OF SYMMETRIC CRACKS AT MID-SPAN. GALERKIN'S AND CHRISTIDE AND BARR'S RESULTS ARE SHOWN FOR VARIOUS CRACK DEPTH RATIO.

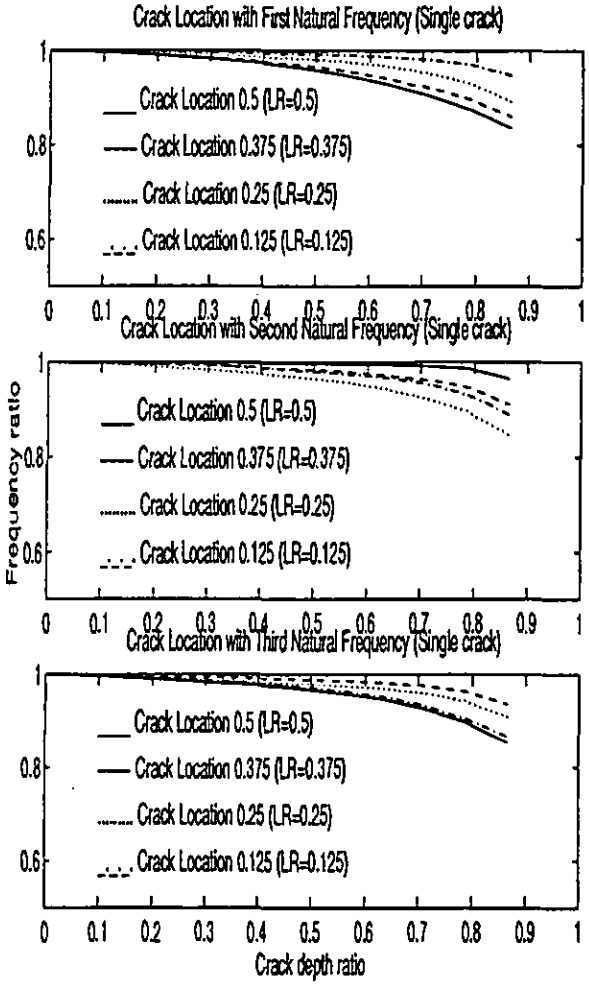

Figure 3: THE FREQUENCY OF A FREE-FREE SHAFT WITH A SINGLE-EDGE CRACK AT DIFFERENT CRACK LOCATIONS.

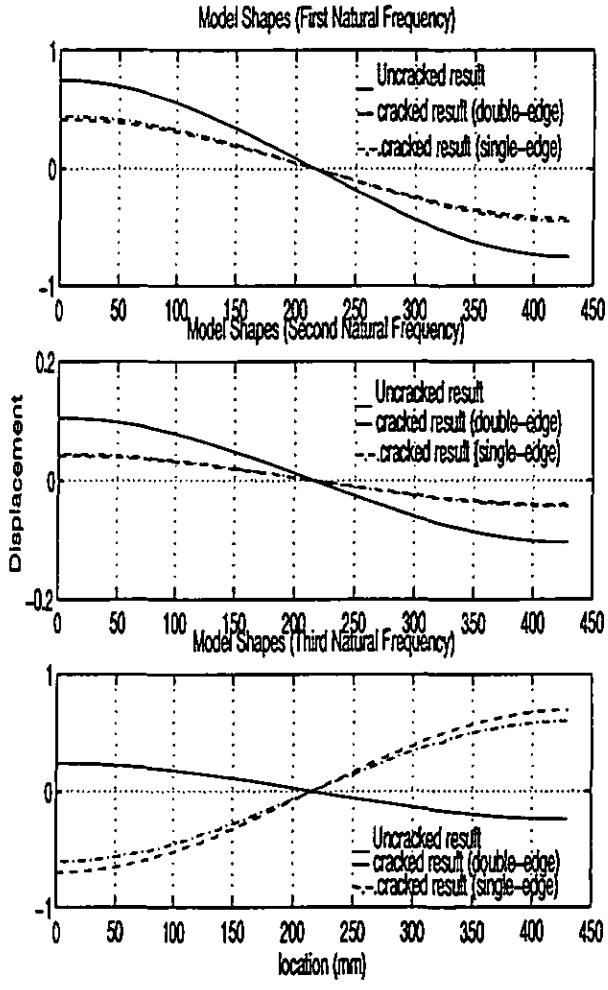

Figure 4: CHANGE IN FIRST MODE SHAPE OF A FREE-FREE SHAFT WITH A PAIR WITH A PAIR OF SYMMETRIC CRACKS AT MID-SPAN (A) DOUBLE-EDGE CRACK (B) SINGLE-EDGE CRACK (C) UNCRACKED.